Fachtagung "Experimentelle Strömungsmechanik"
5.–7. September 2023, München

A method to investigate the transport of dilute bubbles in complex flows

Eine Methode zur Untersuchung des Transports von Blasen geringer Anzahl bei komplexen Strömungsverhältnissen

E. Frense, F. Rüdiger
Institute of Fluid Mechanics, Technische Universität Dresden, 01069 Dresden

Bubble transport, bubble deformation, shadowgraphy, image processing
Blasentransport, Blasendeformation, Schattenverfahren, Bildverarbeitung

Abstract

Current research work at the Institute of Fluid Mechanics at TU Dresden is concerned with the bubble interaction in a joining T-junction channel. Experimental techniques such as the focused shadowgraph method in combination with image processing are mainly used. Due to the rectangular cross-section of the channels and the specific process parameters, the flow in the mixing area is highly three-dimensional, transient and transitional. A first focus of investigation is the description of the shape of deformed bubbles that break up eventually, with particular attention being paid to deformation due to shear in one direction of motion. The bubbles under this strain are primarily stretched or compressed, resulting in a typical shape with axial symmetry along the major axis of the bubbles. With the aim of suitable modelling of the bubble behaviour in the flow, the volume-equivalent diameter proves to be the most suitable characteristic length measure. Due to the complexity of the flow, the simultaneous experimental determination of all quantities relevant for the bubble interaction is almost impossible. Therefore, the second part is dedicated to the qualification and use of numerical simulations for the determination of the variables of the continuous phase at the respective bubble position. This makes it possible, for example, to obtain information about the strain rate as an essential influencing factor for the bubble deformation in the investigated regime.

Zusammenfassung

Ein Forschungsschwerpunkt am Institut für Strömungsmechanik der TU Dresden untersucht die Blaseninteraktion in einem zusammenführendem T-Stück mithilfe experimenteller Messmethoden, wie die fokussierte Schattenbildmethode in Kombination mit Bildverarbeitungsroutinen. Aufgrund des rechteckigen Querschnitts der Stränge und der spezifischen Prozessparameter ist die Strömung im Mischbereich der Zusammenführung stark dreidimensional, instationär und transitionell. Ein erster Untersuchungsschwerpunkt ist die Beschreibung der Größe der sich verformenden Blasen, wobei die Verformung durch Scherung in eine Richtung dominiert. Die Blasen werden unter dieser Belastung primär gestreckt oder gestaucht, was zu einer typischen Form mit axialer Symmetrie entlang der Hauptachse der Blasen führt. Mit dem Ziel einer geeigneten Modellierung des Blasenverhaltens in der Strömung erweist sich der volumenäquivalente Durchmesser als das am besten geeignete charakteristische Längenmaß.

GALA e.V., Karlsruhe, Germany, ISBN 978-3-9816764-9-5

Aufgrund der Komplexität der Strömung ist die gleichzeitige experimentelle Bestimmung aller für die Blaseninteraktion relevanten Größen nahezu unmöglich. Der zweite Teil dieser Arbeit beschreibt daher die Qualifizierung und Nutzung numerischer Simulationen zur Bestimmung der Größen der kontinuierlichen Phase an der jeweiligen Blasenposition. Damit ist es beispielsweise möglich, Informationen über die Scherrate als wesentliche Einflussgröße für die Blasendeformation im untersuchten Regime zu erhalten.

Introduction

The modelling of bubble behaviour is important for several technical applications, because the bubble size spectrum influences important properties of a system. Bubbles can deform according to the exposed stresses which can lead to breakup eventually. Taylor is among the firsts to investigate the deformation of dispersed particles in a continuous phase (Taylor 1934). Other fundamental work has been carried out by Grace 1982. Their research focussed on drops, but nonetheless, for small deformations, bubbles and drops behave similar according to their non-dimensional numbers (Andersson and Andersson 2006). More recently, the deformation of bubbles has been investigated by several authors (Rust and Manga 2002, Müller-Fischer et al. 2008, Taglienti et al. 2023). For small deformation a bubble keeps an ellipsoidal shape which can be described by the deformation parameter

$$D_\mathrm{b} = \frac{l_1 - l_2}{l_1 + l_2} \ , \tag{1}$$

with the bubble major axis length l_1 and minor axis length l_2.
Shear induced deformation is influenced by the shear stress from the liquid phase and the counteracting force due to the surface tension. The ratio of these forces is described with the Capillary number

$$Ca = \frac{\eta_\mathrm{l}\, \dot{\gamma}\, d_\mathrm{b}}{2\, \sigma} \ , \tag{2}$$

with the liquid dynamic viscosity η_l, the strain rate of the continuous phase $\dot{\gamma}$, the bubble diameter d_b and the surface tension σ, respectively. The strain rate is calculated via $\dot{\gamma} = \sqrt{2\, d_{ij}\, d_{ij}}$ with $d_{ij} = 0.5\left(\partial w_i/\partial x_j + \partial w_j/\partial x_i\right)$ from the velocity gradients. For small Capillary numbers ($Ca \ll 1$) and small ratios of the dynamic viscosity of the dispersed, gaseous phase η_g and the dynamic viscosity of the continuous, liquid phase η_l ($\eta_\mathrm{g}/\eta_\mathrm{l} \ll 1$), the bubble deformation depends on the Capillary number only:

$$D_\mathrm{b} = D_\mathrm{b}(Ca) \cong Ca \ . \tag{3}$$

Existing models for bubble interaction and deformation were developed and validated for simplified test cases, where the relevant quantities are well controlled and observable. However, in an industrial context those models are also used for other situations where complex geometries lead to a transient and highly three-dimensional flow field in a transitional regime. In those cases, it can be challenging to calculate a local Capillary number. For example, the bubble diameter can be unknown and must be measured experimentally for example by using image processing. As bubble shapes can get complex due to deformation, the evaluation of the bubble size can yield errors. Therefore, a method is required to derive an equivalent bubble diameter which only to a small extend depends on the deformation. Additionally, quantities

GALA e.V., Karlsruhe, Germany, ISBN 978-3-9816764-9-5

according to the continuous phase at the bubble position are necessary to calculate local characteristic numbers. A method is shown to derive those quantities using a CFD model. The presented routines are tested using an exemplary bubble trajectory where results and limits can be discussed.

Materials and Methods

The object of investigation is a cross-flow type T-junction channel with two inlets and one outlet as illustrated in Fig. 1. Due to flow detachment, a recirculation area is located in the region marked in blue in Fig. 1. The flow configuration considered can be described by the volume flow rate ratio of the two inlet branches $\dot{V}_1/\dot{V}_2 = 2$, and the Reynolds number of the outlet branch $Re_3 = \overline{w}_3\, d_{\mathrm{c,eq}}/\nu_{\mathrm{l}} = 1800$ with the area averaged velocity at the outlet branch 3 $\overline{w}_3$, the hydraulically equivalent diameter of the channel $d_{\mathrm{c,eq}}$ and the kinematic viscosity of the liquid ν_{l}. Bubbles with a pre-defined diameter of $d_{\mathrm{b}} \approx 500\ \mu\mathrm{m}$ are injected at the injection spot marked with a red line in Fig. 1.
The transport of injected bubbles by the flow in a similar configuration is described in Frense et al. 2023. Bubbles get transported towards the region with the dominant velocity gradient which is located at the border between the recirculation zone and the main flow. The dominating component of the shear stress is proportional to $\partial w_x/\partial y$. The flow is assumed to be stationary in this region. Further downstream in the region of the reattachment of the recirculation area in branch 3, the flow is more unstable and more stress components become relevant.

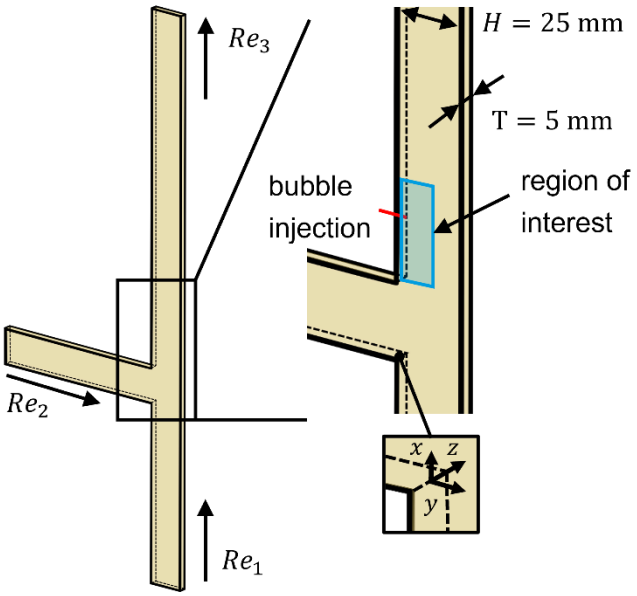

Fig. 1: Sketch of cross-flow type T-junction with two inlets and one outlet branch with location of coordinate system, channel dimensions, bubble injection spot at $x/H = 1.8$ marked with a red line and the region of interest coloured in blue (similar to Frense et al. 2023)

The multiphase flow in the T-junction geometry is investigated with a high-speed shadowgraphy setup which was described in detail in Frense et al. 2023. The greyscale image sequence is evaluated using image processing. Firstly, basic routines were used to generate binary images of the bubbles. The objects of the individual frames get labelled and linked together to one bubble trajectory. Different shape parameters are evaluated for each bubble on each frame of the sequence like the position in the image plane and the absolute value of the depth coordinate position. The latter is derived from the strength of the bubble edge when

GALA e.V., Karlsruhe, Germany, ISBN 978-3-9816764-9-5

using an optical setup with a small the depth of field. This method is described for the hereby used setup in Frense et al. 2022.
Another important interaction parameter is the bubble size. As introduced above, bubbles with a small deformation are simplified as an ellipsoidal body with rotational symmetry around the major axis. Alternatively, the shape can be described as a prolate. Using this assumption, the volume of the body is calculated from the edge line of the projected bubble image. In Fig. 2, the evaluation of the bubble contour is shown for an exemplary image.

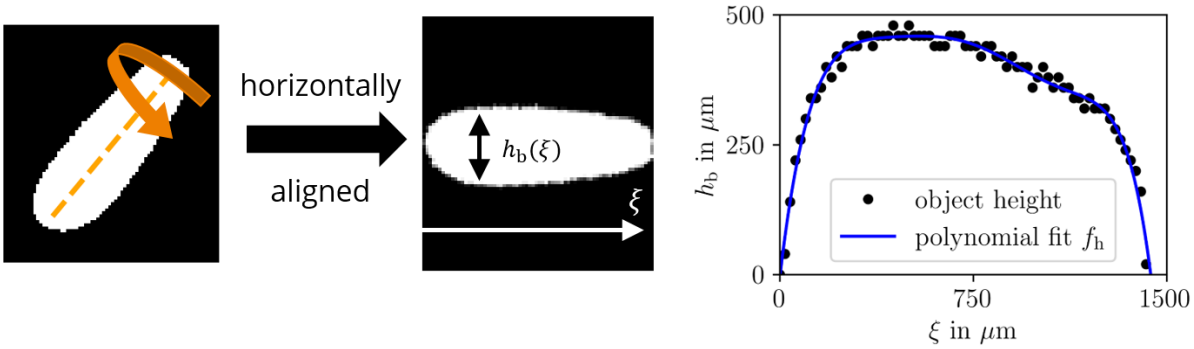

Fig 2: Determination of bubble contour: Exemplary binary image of deformed bubble; horizontally aligned image; extracted bubble height $h_b(\xi)$ and 7th order polynomial fit $f_h(\xi)$ over bubble major axis coordinate ξ

After the horizontal alignment of the bubble's major axis by rotation, the height of the object $h_b(\xi)$ is calculated for every discrete position on the major axis. It should be noted here, that the height is approximately two times the bubble contour radius. As the next step, the volume of the rotational body V_r can be calculated for each frame with

$$V_r = V_r(t) = \pi \int_0^{\xi_{max}} \left(\frac{h_b(\xi)}{2}\right)^2 d\xi \quad . \tag{4}$$

The bubble volume V_b is then derived from one specific frame of the observed trajectory where the bubble has the smallest deformation parameter, therefore

$$V_b = V_r\left(t = t|_{\min(D)}\right) \quad . \tag{5}$$

Additionally, the surface area of the bubble can be calculated using the same assumption. Thus, a 7th order polynomial fit of the bubble height $f_h(\xi)$ was used to calculate the surface area of the rotational body $A_{b,S,r}$ from

$$A_{b,S,r} = \pi \int_0^{\xi_{max}} f_h(\xi) \sqrt{1 + \left(\frac{f_h'(\xi)}{2}\right)^2}\, d\xi \quad . \tag{6}$$

Finally, using the derived bubble volume V_b, it is possible to calculate the volume-equivalent bubble diameter $d_{b,eq,V}$ with

$$d_{b,eq,V} = 2 \sqrt[3]{\frac{3\,V_b}{4\pi}} \quad , \tag{7}$$

GALA e.V., Karlsruhe, Germany, ISBN 978-3-9816764-9-5

which can be interpreted as the diameter of a sphere with the same volume as the rotational body. For comparison, the area-equivalent bubble diameter $d_{\mathrm{b,eq,A}}$ can be evaluated from the projected area of the bubble $A_{\mathrm{b,p}}$ with

$$d_{\mathrm{b,eq,A}} = \sqrt{\frac{4\,A_{\mathrm{b,p}}}{\pi}} \tag{8}$$

and corresponds to the diameter of a circle with the same area of the projected bubble. It is often used in literature as it is easier to evaluate but can potentially yield errors for a deformed bubble.
To obtain the continuous flow parameters, a 3D, laminar, transient CFD model of the single-phase T-junction channel flow was created based on the model described in Frense et al. 2023. The calculations were carried out using ANSYS Fluent 2021 R1. All quantities were averaged over time and exported as the 3D continuous phase flow field data.

Comparison of equivalent bubble diameters

The routine introduced above was applied to an exemplary bubble trajectory. In Fig. 3, the chosen bubble is shown for different states of deformation along the bubble path coordinate s_{b}. The right side of Fig. 3 shows the area and volume-equivalent bubble diameter in grey and black, respectively over the bubble path coordinate s_{b}. The values for the equivalent diameters were evaluated for all frames individually.

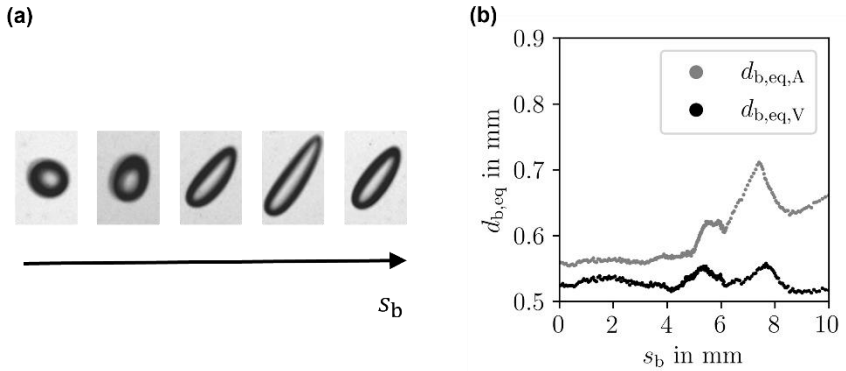

Fig. 3: Equivalent diameter for exemplary trajectory: (a) different stages of bubble deformation selected from trajectory; (b) area-equivalent diameter $d_{\mathrm{b,eq,A}}$ and volume-equivalent diameter $d_{\mathrm{b,eq,V}}$ over bubble path coordinate s_{b}

For the investigated configuration, the conservation of gas volume is assumed because gas exchange between the gaseous and the liquid phase can be neglected. Consequently, every equivalent bubble diameter should stay constant for the bubble trajectory. Any change in the bubble diameter can, therefore, be interpreted as the error of the bubble size determination. For small deformations of the exemplary bubble shown in Fig. 3 in the range of $0 \leq s_{\mathrm{b}} < 5\,\mathrm{mm}$, a slightly bigger value for the area-equivalent diameter compared to the volume-equivalent diameter was found but both values are sufficiently constant throughout. For a higher degree of deformation for $5\,\mathrm{mm} \leq s_{\mathrm{b}} \leq 10\,\mathrm{mm}$, the value of the area-equivalent diameter changes according to the deformation. The relative difference between the maximum

GALA e.V., Karlsruhe, Germany, ISBN 978-3-9816764-9-5

and the minimum diameter is 28 % for this case. In contrary, the volume-equivalent diameter keeps constant to an acceptable extend and the relative difference is below 9 %.

Determination of continuous phase quantities

For the adaption and validation of bubble interaction models several physical quantities are needed but not all can be obtained experimentally in an efficient and convenient way. Because the bubbles are exposed to a highly three-dimensional flow, also 3D information on the flow field must be provided. The most accurate results would be achieved by measuring the bubble and the flow of the surrounding liquid phase, but this would require complex measurement systems. Alternatively, using one-way coupled Euler-Lagrange method as a first approach for numerical modelling, the single-phase flow model of the T-junction channel flow can be used to derive the continuous flow quantities at the bubble position. The scheme to derive necessary quantities is shown in Fig. 4. Image processing can be used to evaluate the shadowgraphy recordings in respect to bubble and bubble interaction parameters. Additionally, the 3D position for each bubble at each frame in known, as described above. The CFD model has been developed to estimate the continuous flow field in the T-junction. PIV measurements have been carried out for verification purposes, but the results are not shown in this work. Altogether, both the bubble and the liquid flow parameters can be derived to adapt or validate bubble interaction models.

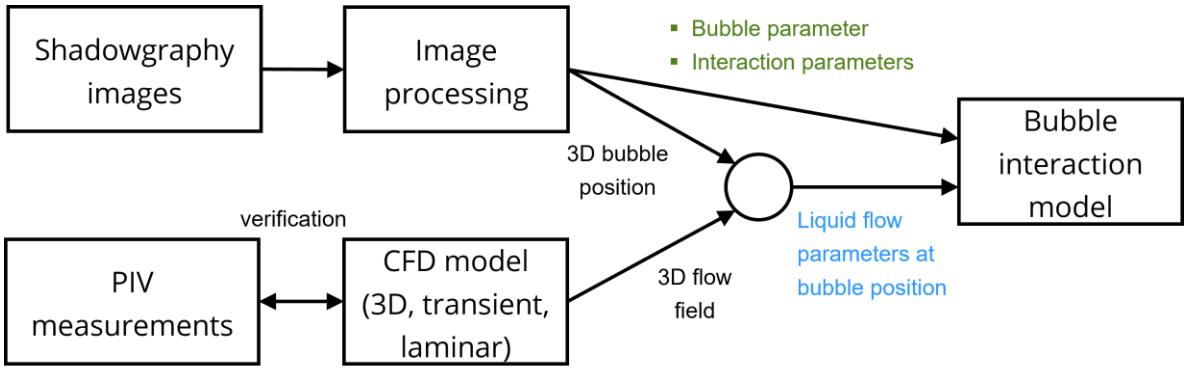

Fig. 4: Method scheme to derive bubble parameters from image processing and flow quantities at the bubble position from a verified CFD model

Several quantities can be derived using this method. For the exemplary bubble trajectory, the deformation parameter D_b is plotted over the bubble path coordinate s_b in Fig. 5a). The strain rate of the continuous phase $\dot{\gamma}$ is extracted at all bubble positions and the Capillary number was calculated using the volume-equivalent bubble diameter $d_{\mathrm{b,eq,V}}$. The Capillary number Ca is plotted over the bubble path coordinate s_b in Fig. 5b). As introduced above, the deformation is assumed to be a result from the exposed stress acting on the bubble surface, described by the Capillary number. Therefore, the values of the deformation parameter are plotted over different Capillary numbers found for the exemplary bubble trajectory in Fig. 5c).
It can be seen in Fig. 5c), that the relation between the deformation parameter and the Capillary number from Eq. 3 show good agreement with the measurements for small deformations of $D_\mathrm{b} \leq 0.3$. Higher deformations yield greater discrepancy. Other functions to describe bubble deformation have been presented in literature but are not discussed in this work.
Some assumptions can yield to errors in the determination of both the quantities. Firstly, the deformation parameter is derived from the 3D bubble shape projected onto the image plane. Further, an ellipsoidal shape is assumed but more complex bubble shapes are not considered. Errors which result from the estimation of the 3D bubble location yield an erroneous shear rate.

GALA e.V., Karlsruhe, Germany, ISBN 978-3-9816764-9-5

Moreover, the shear rate at the bubble centre position must not be the same as the one that is acting along the bubble surface. This yields an error, especially if the spatial change of the shear rate in respect to the bubble size cannot be neglected.

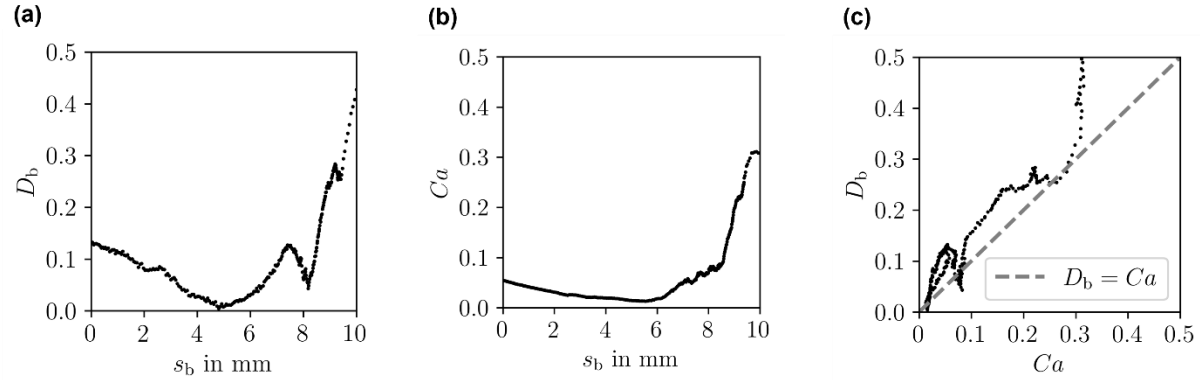

Fig. 5: Deformation due to shear stress for the exemplary bubble trajectory: (a) deformation parameter D_b and (b) Capillary number Ca over bubble path coordinate s_b; (c) deformation parameter over Capillary number and relation from Eq. 3

When discussing the relation between the deformation parameter and the Capillary number, it is presumed that the acting forces yield an immediate deformation without any response time. But because the bubble and the surrounding fluid may act similar to a spring-damper-system, a time-dependent response can be expected when a dynamic change of the strain rate applies to the bubble.
As the bubble gets transported through the T-junction in the experiments, the shear rate acting on the bubbles changes due to the change of the bubble position, but also the time-dependent change of the flow field should be considered. This effect is neglected now due to the temporal averaging of the CFD results but can be relevant in other regions of the T-junction. At the reattachment zone of the recirculation area, the transitional effects are expected to be relevant. Moreover, there are errors from the image processing and the CFD model.

Conclusion

For the adaption and validation of bubble deformation and bubble interaction models several quantities must be determined, which is challenging for complex flow situations. The transport of an exemplary bubble in a T-junction channel flow has been investigated. A relevant physical quantity is the bubble size, which often is described by the area-equivalent diameter but is erroneous for deformed bubbles. A method has been introduced to evaluate the volume-equivalent diameter via the rotation of the bubble contour line around its major axis using image processing. It has been shown that the volume-equivalent diameter is not changing notably for deformed bubbles, which is in in agreement to the conservation of gas volume presumed here. The method is limited to weakly deformed bubbles with axial symmetry and major axis which are straight and not curved. Additionally, errors up to half of an order of magnitude arise when the bubble is not aligned with the image plane.
Furthermore, bubble deformation depends on the local flow quantities, like the strain rate. To measure these quantities in a highly three-dimensional flow field is cost and time consuming. Aa a first approach, one-way coupled Euler-Lagrange numerical simulations is used to model bubble interaction. Therefore, the influence of the bubbles on the surrounding flow field can be neglected. This allows to derive the flow field quantities at the 3D bubble position from numerical simulations of the single-phase flow. The method has been tested for an exemplary bubble

GALA e.V., Karlsruhe, Germany, ISBN 978-3-9816764-9-5

trajectory and potential errors and limitations have been discussed. The relation between the deformation parameter and the capillary number found by Taylor 1984 is in good agreement for a weakly deformed bubble in the investigated configuration. In future work, other quantities of the continuous flow field can be considered. This may be important for regions of the T-junction with a more unstable flow field where dynamic effects have an influence on bubble deformation, but also on bubble interaction. Overall, a well working method has been introduced to reduce the effort for model calibration for complex flow situations which can be found for typical industrial applications.

Literature

Andersson, R., Andersson, B., 2006: “On the breakup of fluid particles in turbulent flows”, AIChE Journal, Vol. 52, No. 6, pp. 2020-2023
Frense, E., Werner, T., Nöpel, J.-A., Rüdiger, F. 2022: “Detection and evaluation of single bubble collisions using focused shadowgraphy”, Proceedings der 29. GALA-Fachtagung "Experimentelle Strömungsmechanik", Ilmenau, pp. 17.1–17.8
Frense, E., Yang, X., Rüdiger, F., Mühlhausen, M.-P., Fröhlich, J., 2023: “Experimental and numerical study on the transport of dilute bubbles in a T-junction channel flow”, Exp. Comput. Multiph. Flow, Vol. 5, No. 4, pp. 396–410
Grace, H. P., 1982: “Dispersion phenomena in high viscosity immiscible fluid systems and application of static mixers as dispersing devices in such systems”, Chem. Eng. Commun., 14, pp. 225-2777
Müller-Fischer, N., Tobler, P., Dressler, M., Fischer, P., Windhab, E. J., 2008: “Single bubble deformation and breakup in simple shear flow”, Exp. Fluids, 45, pp. 917–926
Rust, A. C., Manga, M., 2002: “Bubble Shapes and Orientations in Low Re Simple Shear Flow”, J. Colloid Interface Sci., 249, pp. 476–480
Taglienti, D., Guglietta, F., Sbragaglia, M., 2023: “Reduced model for droplet dynamics in shear flows at finite capillary numbers”, Phys. Rev. Fluids, 8, 013603
Taylor, G. I., 1934: “The formation of emulsions in definable fields of flow”, Proc. R. Soc. Lond. Ser. A, 146, pp. 501-523

GALA e.V., Karlsruhe, Germany, ISBN 978-3-9816764-9-5